Curved and Layer. Struct. 2016; 3 (1):214–222 DE GRUYTER OPEN

Research Article Open Access

S. Shevtsov*, I. Zhilyaev, P. Oganesyan, and V. Axenov

Material Distribution Optimization for the Shell Aircraft Composite Structure

DOI 10.1515/cls-2016-0017
Received May 26, 2016; accepted Jun 10, 2016

Abstract: One of the main goal in aircraft structures designing is weight decreasing and stiffness increasing. Composite structures recently became popular in aircraft because of their mechanical properties and wide range of optimization possibilities. Weight distribution and lay-up are keys to creating lightweight stiff strictures. In this paper we discuss optimization of specific structure that undergoes the non-uniform air pressure at the different flight conditions and reduce a level of noise caused by the airflow-induced vibrations at the constrained weight of the part. Initial model was created with CAD tool Siemens NX, finite element analysis and post processing were performed with COMSOL Multiphysics® and MATLAB®. Numerical solutions of the Reynolds averaged Navier-Stokes (RANS) equations supplemented by k-w turbulence model provide the spatial distributions of air pressure applied to the shell surface. At the formulation of optimization problem the global strain energy calculated within the optimized shell was assumed as the objective. Wall thickness has been changed using parametric approach by an initiation of auxiliary sphere with varied radius and coordinates of the center, which were the design variables. To avoid a local stress concentration, wall thickness increment was defined as smooth function on the shell surface dependent of auxiliary sphere position and size. Our study consists of multiple steps: CAD/CAE transformation of the model, determining wind pressure for different flow angles, optimizing wall thickness distribution for specific flow angles, designing a lay-up for optimal material distribution. The studied structure was improved in terms of maximum and average strain energy at the constrained expense of weight growth. Developed methods and tools can be applied to wide range of shell-like structures made of multilayered quasi-isotropic laminates.

Keywords: laminated composites; aircraft design; structural optimization

1 Introduction

Optimization of composite structures was studied by number of scientific and engineering groups during last years. Some approaches and methods were developed to create partially automated process of designing optimal composite structures. Most of these methods and appropriate modeling and optimization tools that are developed by the leading scientific groups [1–3], basically, for aircraft applications, started from the first attempts of structural optimization [4], which have been then actualized in fundamental monographs, especially dedicated to the problems of composites mechanics, design and technology [5–7]. As the objective or merit function, most optimization methods should provide the highest stiffness to-weight ratio [8, 9], maximization of the first natural frequencies or minimization of the equivalent stress due to various stress hypotheses [10] at the constrained part volume (weight), and sometimes, at the restriction on the optimized external or internal shape, manufacturing constraints like lower and upper bound thickness on the laminate, or number of successive plies of same orientation. Anisotropic materials induce a lot of additional optimization parameters, including wall thickness distribution, orientation and stacking sequence, stiffener spacing and location.

The modern view on the non-homogeneous structures optimization process, which is characterized as the simultaneous design and optimization, assumes that it includes the main three phases [2, 3]. On the first phase on conceptual design that is called the free-size or topology optimiza-

***Corresponding Author: S. Shevtsov:** South Center of Russian Academy, 344006, Tchekhov str., 41, Rostov on Don, Russia; Southern Federal University, 344090, Milchakov str., 8A, Rostov on Don, Russia; Email: sergnshevtsov@gmail.com
I. Zhilyaev: South Center of Russian Academy, 344006, Tchekhov str., 41, Rostov on Don, Russia; Southern Federal University, 344090, Milchakov str., 8A, Rostov on Don, Russia; Email: zhilyaev@mail.com
P. Oganesyan: Southern Federal University, 344090, Milchakov str., 8A, Rostov on Don, Russia; Email: gwolwer1ne@gmail.com
V. Axenov: Mil Moscow Helicopter Plant, Rostov Branch, 344038, Novatorov str., 5, Rostov on Don, Russia; Don State Technical University, 344000, Gagarin sq., 1, Rostov on Don, Russia; Email: vnaxenov@mail.ru

tion, the total laminate thickness and the optimal composition of the composite laminate can change 'continuously' throughout the structure [3]. At the second phase of the detailed design when ply bundle sizing is implemented by ply-based finite element (FE) modeling, the thickness of each ply bundle vary to optimize all objectives considering the manufacturing constraints and restrictions, and these ply thicknesses for each simulated structure form the coordinates of vector in the design space. Third phase of the simultaneous design and optimization [2, 3] consists of a shuffling (redistribution) process to determine the optimal stacking sequence, while also satisfying additional manufacturing constraints, such as providing balance of laminate [6, 7]. These three phases present in the most common case of design, but many aircraft parts, such as radomes and cowlings that have open shell geometry and are manufactured using quasi-isotropic laminates, which have the same Young's modulus Y and same Poisson's ratio v in all in-plane directions, but not normal to the plane [6–9, 11]. Such quasi-isotropic laminates can be produced when the following rules are satisfied [6]:

1. The total number of unidirectional layers must be n ≥ 3.
2. All layers must have identical orthotropic elastic constants and identical thickness.
3. The orientation of the k-th layer of a n-layered laminate is $\theta_k = \pi \cdot (k-1)/n$.

These aircraft parts are manufactured using open mould technology when prepregs are applied to the mould (male or female) surface layer by layer depending on the desired thickness distribution [7, 12]; then composite part is cured in autoclave under a vacuum bag. The case of quasi-isotropic material is much simpler than the common case of three phase optimization, because it allows to consider the material of optimized structure as isotropic [13, 14].

Most real world structural optimization problems require a CAD model of the structure to be optimized, which further is converted to the FE representation [1–3, 10, 15, 16]. Usually, modeling of quasi-isotropic laminates excludes from consideration architecture of the reinforcement (unidirectional roving, woven fabrics, braids, etc.); on the contrary, the properties of composite materials are accepted as homogenized, which were previously determined experimentally or numerically using the representative volumes [14, 17]. In order to determine the stress-strain state in the most stressed area of the optimized part, a forward problem for the given boundary conditions and the operating load cases is formulated, and FE simulations are carried out, sometimes, by using means for numerical CFD analysis [1, 3, 10].

The optimization algorithm that can be based on the known topology optimization methods and their recent improvements [10, 18–20], which are inherent a great number of degrees of freedom (design variables), or methods, which imply a finite number of varied parameters, *e.g.*, genetic algorithms [11, 16, 21] and artificial neural networks [16]. These last ones require some parameterization, *i.e.*, conversion of problem to the finite number of design variables. It can be implemented representing the part geometry by an analytical function, whose parameters become the design variable [22], by a pointwise presentation of the material's distribution over the structure [23, 24], or by the gauge optimization models where whole part is divided onto 10 and more distinct zones, which are optimized separately [2, 3, 8].

If we would like to optimize for more than one objective function at the same time, *e.g.*, performance and cost, or both mass and compliance objectives, a Pareto approach is the most efficient for such the problems [3, 5, 7, 11, 16, 18].

Once the composite shell-like structure is optimized, the ply orientation on a mould surfaces with bi-directional curvature need to be determined by a draping analysis [2, 7, 15]. To eliminate excess cloth and its shear deformation when a ply is placed over the curved mould surface, darts (cuts of roving or fabric) need to be placed. A kinematic or mapping approach to the problem of draping, which is used here, assumes a geometric mechanism to transform an initial unit square of fabric into the corresponding draped shape at such assumptions [15]:

- The yarns are inextensible in the fiber direction.
- Tool-ply and ply-ply friction is neglected.
- Crossover points of warp and weft yarns act as pivoting joints for woven fabric, or the transverse spacing between fibers is constant for unidirectional materials.
- The composite ply maps perfectly onto the tool surface without out-of-plane wrinkles or discontinuities.
- The manufacturing process (hand lay-up in the considered case) defines how the composite sheet is "pinned" onto the tool surface.

There are some CAD and highly targeted software [2, 15], but because even a part created on a very simple and smooth mould surface can produce a final volume with complex geometry, it is very difficult to adequately model these darts location using draping soft tool in CAD systems. It is a good practice to allocate darts on the part sur-

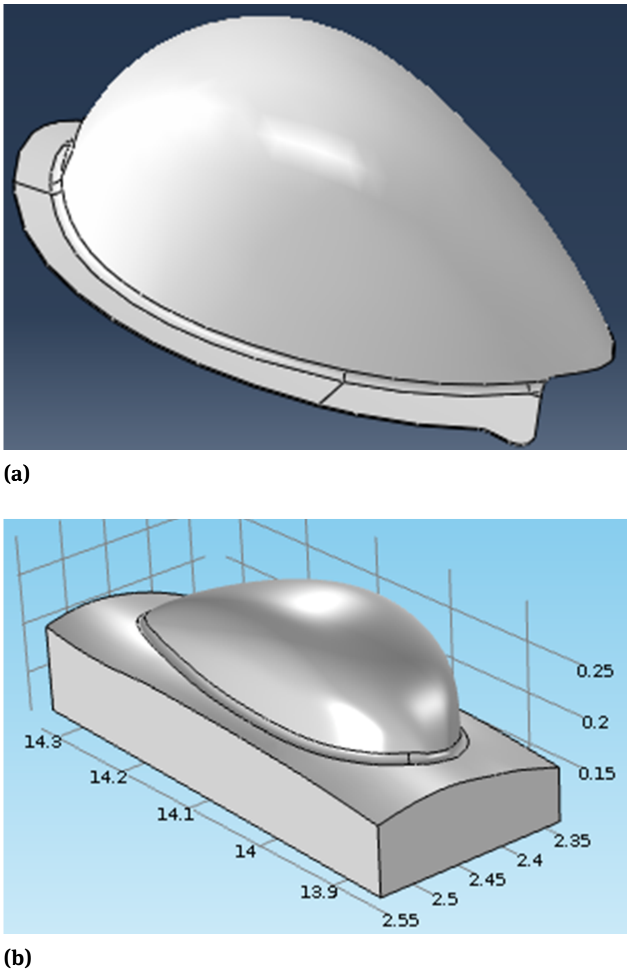

Figure 1: Geometry of the cowling imported form CAD model (a) and its transformation to the external surface of stiff 3D body (b).

faces with the smallest curvature; and these darts should be spatially separated from each other.

This paper is targeted to the problem of structural optimization of rotorcraft radar cowling, which has geometry like open shell and undergoes the spatially distributed transient pressure from the airflow at the climbing / descent (±10 deg) modes of flight with a speed 300 km/h. Optimization target is to minimize the total strain energy and reduce maximum von Mises stress values. The total strain energy is equivalent to the mean compliance of the structure. First, we convert the CAD model of the cowling to FE representation of its external surface assumed as a stiff shell; and air blasting in a wind tunnel of this shell was simulated at the different orientation of airflow to find the most stressed mode of flight. This direct problem was numerically solved using Navier-Stokes equations averaged by Reynolds technique and supplemented by k-w turbulence model. The results of the FE model transient analysis were the spatial distributions of air pressure acting to the shell surface. On the next step we solve the structural dynamics problem for this shell loaded by newly found pressure field. The shell is made of quasi-isotropic material with a variable wall thickness, which is controlled by four design variables. We proposed the simple parameterization of the problem, which introduces an auxiliary sphere with varied radius and coordinates of the center that are used as the design variables. Curve that formed by the intersection of the shell with sphere defines some boundary of area, where the shell walls should be stiffened by local thickening. To eliminate a local stress concentration this increment was defined as the smooth function defined on the shell surface. The optimization algorithm performs a direct search of optimum design inside a subset of 4D design space at constrained maximum wall thickness and total weight of the part, calling the forward problem for the most stressed loading case. The maximum strain energy in the optimized cowling was reduced by 73% at the weight growth up to 54%, whereas the eigenfrequencies at the 6 first natural vibration modes have been increased by 10–15%.

As a technological result of structural optimization we obtained the thickness of shell walls distribution, which then was used to design the draping of composite prepreg. Shell surface with two kind of perpendicular geodesic lines were deployed on the plane to obtain the draped shape of composite sheets lay-up.

2 Methods

It is a common case in aircraft design to use shell-like glass-fiber epoxy based composite cowlings that are mounted on the stiffer part of airframe. These cowlings undergo a transient action of airflow that can cause undesirable deformations, mechanical vibrations and noise. To determine the spatial distribution of air pressure on the shell surface we neglected by a fluid-structure interaction, and supposed the shell as non-deformable, stiff body, which external surface has the shape like the studied shell (see Fig. 1). All cowling dimensions were assumed small with respect to dimensions of airframe. Hence, CAD model of the studied cowling was imported to Comsol Multiphysics software using Comsol's built-in CAD import converter, then all side surfaces were extruded on the distances that were sufficiently large than dimensions of cowling.

The problem has been formulated by using the Reynolds averaged Navier-Stokes (RANS) equations [25]. We use $k-\omega$ turbulence model that behaves better close to walls and usually predicts free shear flows more accurately than the k–ε model. The k–ω turbulence model with two additional equations for the turbulent kinetic energy k and for the dissipation per unit turbulent kinetic energy, ω was a closure of RANS equations, which model transport of turbulent kinetic energy k and ω

$$\begin{cases} \rho\frac{\partial k}{\partial t} + \rho\mathbf{u}\cdot\nabla k = \frac{1}{2}\mu_T\left(\nabla\mathbf{u} + (\nabla\mathbf{u})^T\right)^2 \\ \qquad +\nabla\cdot\left[\left(\mu + \sigma^\star\mu_T\right)\nabla k\right] - \rho\beta^\star k\omega \\ \rho\frac{\partial\omega}{\partial t} + \rho\mathbf{u}\cdot\nabla\omega = \frac{\alpha}{2}\mu_T\frac{\omega}{k}\left(\nabla\mathbf{u} + (\nabla\mathbf{u})^T\right)^2 \\ \qquad +\nabla\cdot\left[\left(\mu + \sigma\mu_T\right)\nabla\omega\right] - \rho\chi\omega^2 \end{cases} \tag{1}$$

where the previous equations use the following closure constants and functions.

$$\alpha = \frac{13}{25};\quad \beta = \beta_0 f_\beta;\quad \beta^\star = \beta_0^\star f_\beta;\quad \sigma = \frac{1}{2};\quad \sigma^\star = \frac{1}{2} \tag{2}$$

$$\beta_0 = \frac{9}{125};\quad f_\beta = \frac{1+70\chi_\omega}{1+80\chi_\omega};\quad \chi_\omega = \left|\frac{\Omega_{ij}\Omega_{jk}S_{ki}}{\left(\beta_0^\star\omega\right)^3}\right| \tag{3}$$

$$\beta_0^\star = \frac{9}{100};\quad f_{b^\star} = \begin{pmatrix} 1 & \chi_k \le 0 \\ \frac{1+680\chi_k^2}{1+400\chi_k^2} & \chi_k > 0 \end{pmatrix};$$
$$\chi_k = \frac{1}{\omega^3}\left(\nabla k\cdot\nabla\omega\right) \tag{4}$$

The tensors Ω_{ij} and S_{ij} are the mean rotation-rate tensor and the mean strain-rate tensor, respectively, defined by

$$\Omega_{ij} = \frac{1}{2}\left(\frac{\partial\bar{u}_i}{\partial x_j} - \frac{\partial\bar{u}_j}{\partial x_i}\right)\quad S_{ij} = \frac{1}{2}\left(\frac{\partial\bar{u}_i}{\partial x_j} + \frac{\partial\bar{u}_j}{\partial x_i}\right) \tag{5}$$

and the turbulent viscosity is

$$\mu_T = \rho\frac{k}{\omega} \tag{6}$$

In order to determine the velocity field and the total pressure distribution along the wall of a cowling's model we used the transient formulation of the turbulence flow problem when airspeed in inlet started from zero velocity, slowly increased then reached its steady value ~83 m/s (300 km/h), which corresponds to the helicopter cruise speed. In outlet a boundary condition was assumed as $p = 0$, whereas conditions in the form of the wall functions

$$\begin{cases} \mathbf{u}\cdot\mathbf{n} = 0 \\ u_{\tan} = \mathbf{u} - (\mathbf{u}\cdot\mathbf{n})\,\mathbf{n} \end{cases} \tag{7}$$

where $\mathbf{n}$ is unit normal to a wall, were used on the walls of the wind tunnel and also on the surface of cowling that assumed as absolutely stiff.

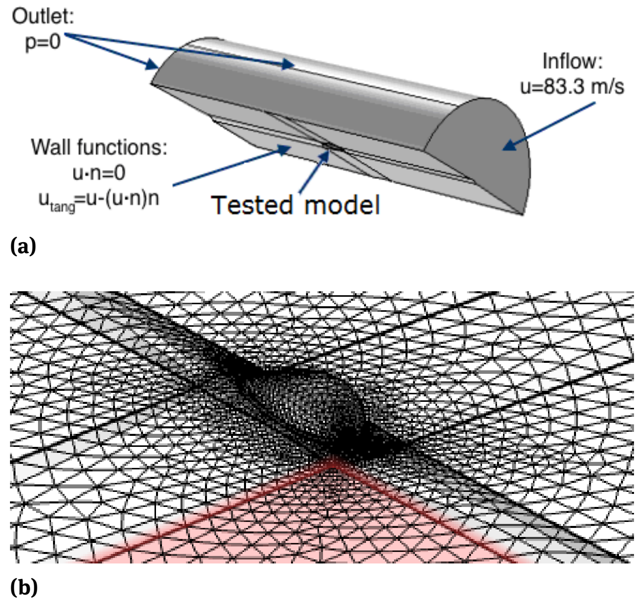

Figure 2: Geometry (a) and finite element meshing (b) at the virtual wind tunnel test of the cowling.

During a virtual test, the model has been placed in the semicircular test section of the tunnel at the different model orientation relative to airflow, which is aligned with the tunnel axis. The finite element mesh for the air volume consisted of near 90 000 tetrahedron elements (see Fig. 2).

The transient problem has been solved for the angles within a range ±10 deg of the tested model orientation relative to the tunnel axis, with a step of 2.5 deg. The spatial distributions of the pressure field, which acts on the model surface (see Fig. 3), were stored in the text files for the further numerical processing.

At the stage of stress/strain state determination for the studied shell, its material vas modeled as isotropic. The elastic properties for the quasi isotropic materials were accepted for the multilayered composite manufactured by laying-up of a fabric prepreg with the Young module $2\cdot10^{10}$ Pa, Poisson ratio 0.3 and density 2200 kg/m^3. The finite element formulation of the forward problem uses the shell model for the cowling structure (see Fig. 4) with homogenous wall thickness of 2.5 mm. Its geometry is transformed from the CAD model. Volume of the cowling before optimization is $1.46\cdot10^{-4}$ m^3, and weight is 0.652 kg.

The total elastic strain energy of the shell we used as the objective function; it was calculated at the solving the forward problem, when the shell surface has been loaded by non-uniform quasi static pressure field determined at the previous study. The values of these energies are shown in Table 1, which demonstrates that the most stressed case

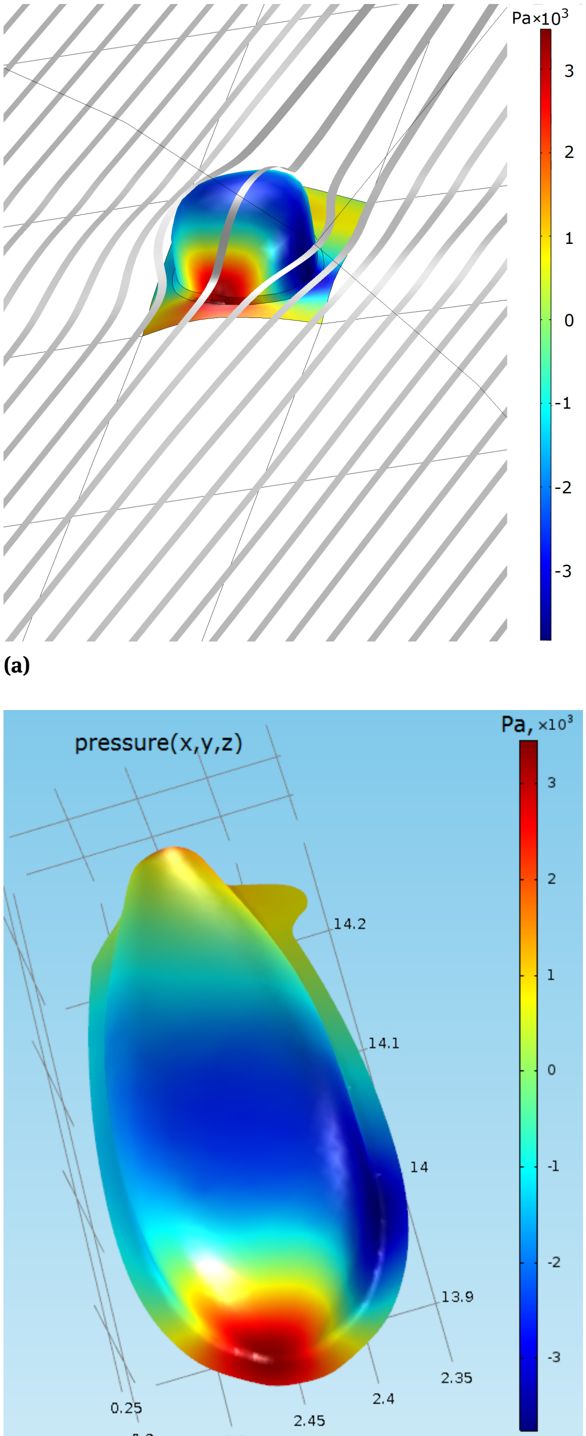

Figure 3: The examples of streamlines map (a) and pressure distribution on the model surface (b).

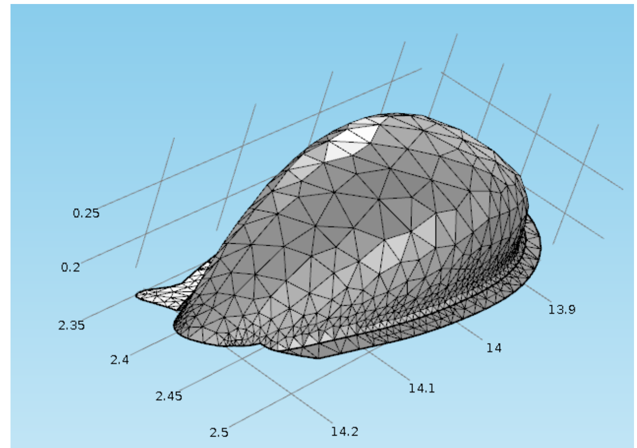

Figure 4: Model's geometry and finite element mesh at the solving of the forward problem for optimized cowling.

Table 1: The elastic strain energy (×10^{-6} J) of the shell blowing at the different angles (deg).

−10	−5	0	+5	+10
27.6	23.7	22.1	20.8	20.6

corresponding to the value −10 deg of the airflow orientation.

Our attempts to apply known topology optimization methods, such as SIMP [19], ESO, BESO [20] to optimize the shell's thickness distribution were unsuccessful due to formation of stillbirths structures and very low stability. Topology of the presented shell is not supposed to have any additional cavities or holes, therefore, we decided to parameterize the problem and by this way reduce the dimensionality of the design space. An artificial technique has been proposed to parameterize this problem. This technique introduces the fictive sphere, which intersection with the shell surface circumscribes the area of the shell where its thickness should be optimized (see Fig. 5). The spatial distribution of the shell thickness in this area is given by a smooth function of 4 design variables $K\,(x_p, y_p, z_p, R)$

$$\begin{cases} h = h_0(K+1) \\ K = \begin{cases} 0, D > R \\ \left((\mathrm{R}-\mathrm{D})/\mathrm{R}\right)^2 \end{cases} \\ D = \sqrt{(x-x_p)^2 + (y-y_p)^2 + (z-z_p)^2} \end{cases} \tag{8}$$

where h_0 = 2.5 mm is the initial thickness of the shell that adopted unchanged before optimization, x_p, y_p, z_p and R are the coordinates of center and radius of the auxiliary sphere, respectively.

Due to instability in current case we didn't used direct bult-in Comsol optimization algorithms. Instead, numerical experiment was held a series of forward problems with parametrized parameters. The workflow of optimization, implements a cyclic call of the forward problem, whereby

Table 2: The best optimization results compared with the initial design properties (for the blowing angle −10 deg).

Shell's design	Design variables				Weight, kg	Total strain energy, J	Max strain energy, J/m^3	Max Von Mizes stress, MPa
	x_p, m	y_p, m	z_p, m	R, m				
Not optim.	NA	NA	NA	NA	0.652	$8.87 \cdot 10^{-5}$	17171	0.887
Optimum design A	14	2.41	0.22	0.5	1.023	$3.81 \cdot 10^{-5}$	4183	0.516
Optimum design B	14	2.41	0.23	0.5	1.026	$3.80 \cdot 10^{-5}$	4185	0.516
Optimum design C	14	2.38	0.22	0.5	1.010	$3.82 \cdot 10^{-5}$	4511	0.524

Note: The coordinates x_p, y_p, z_p are given in the aircraft frame

Table 3: First three eigenfrequencies before and after optimization (for the blowing angle −10 deg).

Shell's design	Frequency 1, Hz	Frequency 2, Hz	Frequency 3, Hz
Not optim.	818.22	1189.7	1317.1
Optimum design A	902.49	1324	1683.8
Optimum design B	902.49	1324	1683.8
Optimum design C	899.61	1317.6	1689.1

Table 4: The best optimization results for the optimized designs A, B, and C at the blowing angle +10 deg).

Shell's design	Total strain energy, J	Max strain energy, J/m^3	Max Von Mizes stress, MPa
Not optim.	$6.84 \cdot 10^{-5}$	12227	0.798
Optimum design A	$2.89 \cdot 10^{-5}$	1953	0.549
Optimum design B	$3.8 \cdot 10^{-5}$	1197	0.516
Optimum design C	$2.94 \cdot 10^{-5}$	2221	0.570

the domain in the space of design variables has been uniformly covered with the points corresponding to different sets of parameters x_p, y_p, z_p, R, and this domain is mapped to the objective space. The optimization results have been stored in the form of tables and text files, which contain the spatial thickness distributions for each set of design variables. All designs that didn't satisfied constraint on the cowling weight $W \leq 1.2$ kg are not considered. The total number of simulated variants for angle −10 deg exceeds 500. The values of total strain energy combined with the values of the mass shell for the entire set of considered design variants are presented in Fig. 6.

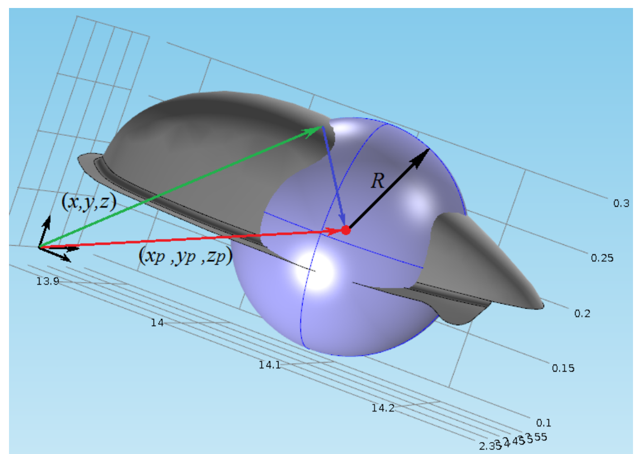

Figure 5: Defining the design variables for the problem of the shell optimization.

3 Results

Three best solutions of the optimization problem are present in Tables 2 and 3, where they are combined with the values of total and maximum strain energies for not optimized shell.

We also tested selected parameters combinations against flow angle 10 deg to proof that these results not only suitable for one airflow direction. Results are presented in Table 4.

In order to reconstruct the spatial wall thickness distribution within the shell surface we unwrapped this surface using MATLAB script, whose input is any text file obtained during optimization. As the origin of the laminate pattern coordinate frame we used the upper point of the cowling. The deployment algorithm performs a cyclic incision of

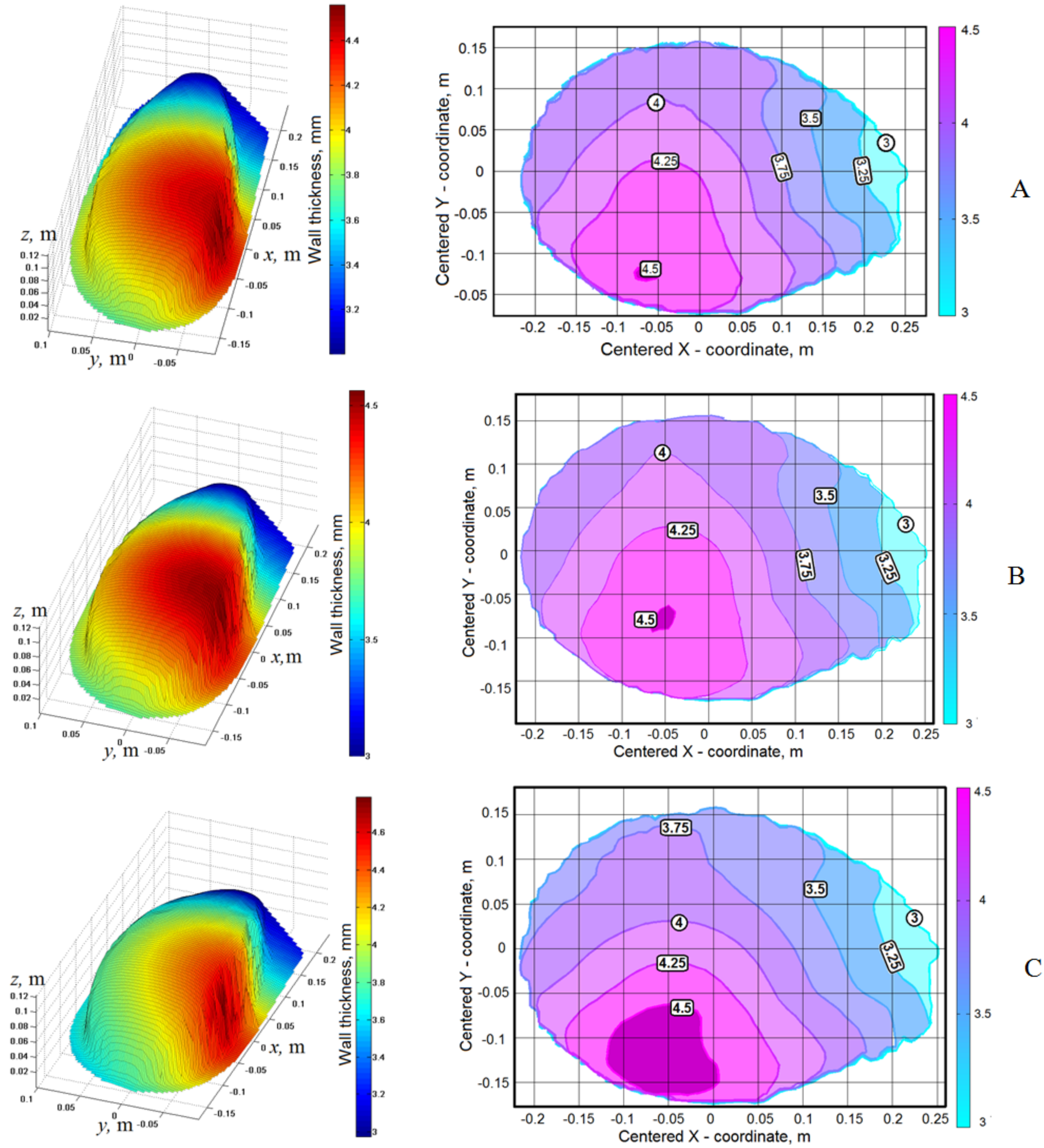

Figure 6: Three spatial thickness distributions within the surface of optimized shell (left) and corresponding patterns of lay-up (right).

the shell surface by the vertical planes that pass through a vertical coordinate axis of new frame. These planes are turned around this axis in the range $\phi \in [0; 360]$ deg with the angular step $\Delta\phi = 5$ deg. The lengths of the section lines $z\,(x\,(r,\phi)\,,y\,(r,\phi))$ are numerically integrated using formula

$$l\,(r,\phi) = \int\limits_{r} \sqrt{1 + \left(z'_r(r,\phi)\right)^2}dr \tag{9}$$

where polar coordinate r are determined in the area, which is occupied by the shell. Thereby, these lengths allow implementing mapping $(r,\phi) \rightarrow (l,\phi)$ and expressing the wall thickness distribution as a function of the new coordinates $h\,(r,\phi) \rightarrow \tilde{h}\,(l,\phi)$, which is defined on (l,ϕ) plane. The numerical interpolation of $\tilde{h}\,(l,\phi)$ and its graphical representation by the set of level lines permits to construct the pattern of lay-up (see Fig. 6). The level lines with a step of 0.25 mm thickness (two prepreg layers) allow to easily optimizing a final stacking sequence by shuffling the plies oriented according to the scheme [0^0; 90^0; $+45^0$; -45^0]. The problem of the rational darts placement was not considered because of poorly substantiated assumption about inextensible prepreg's fabric [2, 7, 15].

4 Discussion

Presented approach consists of three independent steps. First, we obtain a distribution of pressure on the surface of the studied structure using $k-\omega$ turbulence model. Further, we parameterize the structural optimization problem by the artificial method, which is suitable for curved shell-like structures; and perform the optimization procedure. For presented structure the optimal solution provides a decrease in more than two times of the global stain energy, a reduction of the peak von Mizes stress of 40%, and 10–20% growth of the vibration frequencies on the first six natural modes. Finally, we construct the lay-up of prepreg using mapping method to unfold the fiber-reinforced composite sheets placed on a double curvatures surface of the mould. Presented method can be used for wide range of shell-like parts and allows to significantly improving the mechanical properties that are important in aircraft, spacecraft and rotorcraft structures: weight, structural stiffness, peak stress, and vibration frequencies.

Acknowledgement: This research was supported by the Russian Foundation for the Basic Research (Grant 15-08-00849) and by the Russian Academy of Science (Project 0256-2015-0074).

References

[1] Ostergaard M. G., Ibbotson A. R., Le Roux O. and Prior A. M., Virtual Testing of Aircraft Structures, CEAS Aeronaut. J., 2011, 1, 83–103
[2] Zhou M., Fleury R. and Kemp M., Optimization of Composite: Recent Advances and Application, 2011, www.altairproductdesign.com
[3] Rao J. S., Advances in Aero Structures, In Proceedings of ICOVP-2015 Conference (Guwahati, India, 2015), 20
[4] Haug E. J. and Arora J. S., Applied Optimal Design: Mechanical and Structural Systems, John Wiley &Sons, N.-Y., 1979
[5] Jones R. M., Mechanics of Composite Materials, Taylor & Francis, Inc., Philadelphia, 1998
[6] Staab G. H., Laminar Composites, Butterworth-Heinemann, Wobum, MA, 1999
[7] Baker A., Dutton S. and Kelly D., Composite Materials for Aircraft Structures, AIAA Eds., Virginia, 2004
[8] Yancey R. N. and Stefanovic M., A Practical Method to Meet the Composite Optimization Challenge, 2013, www.altairproductdesign.com
[9] Kress G., Design Criteria, In: Composites. ASM Handbook, Vol. 21, ASM International, Materials Park, OH, 2001
[10] Meske R., Sauter J. and Zeynel G., Recent Improvements in Topology and Shape Optimization and the Integration into the Virtual Product Development Process, In: Proceedings of International Workshop on Advances in Shape and Topology Optimization, Graz, Austria, 2008
[11] Gillet A., Francescato P. and Saffre P., Single- and Multi-objective Optimization of Composite Structures: The Influence of Design Variables, J. of Compos. Mater., 2010, 44, 457–480
[12] Kaynak C. and Akgül T., Open Mould Processes, In: Akovali G. (Ed.) Handbook of Composite Fabrication, RAPRA Technology Ltd., Shawbury, UK, 2002
[13] Cumming W. D. et al., Multidirectional Tape Prepregs, In: Composites. ASM Handbook, Vol. 21, ASM International, Materials Park, OH, 2001
[14] Thomas H. L., Zhou M., Shy Y. K. and Pagaldipti N., Practical Aspects of Commercial Composite Topology Optimization Software Development, In: Rozvany G. I. N. and Olhoff N. (Eds.), Topology Optimization of Structures and Composite Continua, Kluver Academic Publishers, Dordrecht, Boston, London, 2000
[15] Guillermin O., Computer-Aided Design and Manufacturing, In: Composites. ASM Handbook, Vol. 21, ASM International, Materials Park, OH, 2001
[16] Vosniakos G.-C., Maroulis T. and Pantelis D., A method for optimizing process parameters in layer-based rapid prototyping, Proc. Inst. of Mech. Eng., Part B: J. Eng. Manufact., 2007, 221, 1329–1340
[17] Rastogi N., Finite Element Analysis, In: Composites. ASM Handbook, Vol. 21, ASM International, Materials Park, OH, 2001
[18] Querin O. M., Steven G. P. and Xie Y. M., Advances in Evolutionary Structural Optimization: 1992-2000, In: Rozvany G. I. N. and Olhoff N. (Eds.), Topology Optimization of Structures and Composite Continua, Kluver Academic Publishers, Dordrecht, Boston, London, 2000
[19] Bendsoe M. P. and Sigmund O., Topology Optimization. Theory, Methods and Applications, 2nd ed. Springer, Berlin, 2004
[20] Huang X. and Xie Y. M., Evolutionary Topology Optimization of Continuum Structures: Methods and Applications, John Wiley &Sons, Chichester, UK, 2010
[21] Gyan S., Ganguli R. and Naik G. N., Damage-tolerant design optimization of laminated composite structures using dispersion of ply angles by genetic algorithm, J. of Reinf. Plast. and Compos., 2012, 31, 799–814
[22] Shevtsov S. et al., Dynamics of Power High-Stroke Flextensional PZT Actuator with Optimized Shell. Numerical and Experimental Study, In Proceedings of the European Conference on Structural Dynamics – EURODYN-2014 (Porto, Portugal), 1631–1638
[23] Taylor J. E., A Formulation for Optimal Structural Design with Optimal Materials, In: Rozvany G. I. N. and Olhoff N. (Eds.), Topology Optimization of Structures and Composite Continua, Kluver Academic Publishers, Dordrecht, Boston, London, 2000
[24] Oganesyan P., Zhilyaev I., Shevtsov S. and Wu J.-K., Optimized Design of the Wind Turbine's Composite Blade to Flatten the Stress Distribution in the Mounting Areas, In: Dynybyl V. et al. (Eds.), The Latest Methods of Construction Design, Springer Verlag, 2015

[25] Wilkes J. O., Fluid Mechanics for Chemical Engineers with Microfluidics and CFD, 2nd ed. Prentice Hall International Series in the Physical and Chemical Engineering Sciences, Westford, MA, 2012